Chapter 3

Solar Cell I-V Characteristics

It is well known that the behaviour of a PhotoVoltaic (PV) System is greatly influenced by factors such as the solar irradiance availability and distribution and temperature. Before analysing the PV generator behaviour under non-ideal condition, i.e., with partial shading, an accurate model of the solar cell is required to study it under ideal conditions.

3.1 Single diode model for solar cell

The PhotoVoltaic (PV) effect [45] is the physical basis for the conversion of the solar radiation absorbed by a solar cell to the resulting generated current. Avoiding the particulars, beyond the aim of this dissertation, a silicon (Si) semiconductor mono-junction solar cell is basically a large[1] p-n junction, obtained with an n-type Si region (doped with atoms of donor elements for Si), typically the emitter, and a p-type Si region (doped with atoms of acceptors elements for Si). If this structure is exposed to a radiation whose quantum energy is higher than the Si energy gap (1.12 eV), then the photo-generated electron-hole pairs can be separated by the electric field present in the junction and reach the metallic electrode, if this is within the charge carrier diffusion length or if other recombination mechanisms don't occur. The charge carrier generation has the same effect of a direct polarization on the p-n junction, so the potential barrier decreases and

[1] Large compared with other electronic devises, i.e., with a 15.6 x 15.6 cm^2 surface for a typical polycrystalline silicon cell.

more diffusion of minority carrier occurs in both the p-type and n-type regions, until another equilibrium state is reached. The generated current by a solar cell is therefore dependent mainly on the incident solar irradiance, the medium spectral response, which comprehends its External Quantum Efficiency (EQE) and, so, the generation-recombination effects, and its illuminated area. Thus a solar cell can be modelled as a current source, whose generated photocurrent is independent from the load and can be expressed as [46]

$$I_{ph} = K_s \cdot G \cdot A \tag{3.1}$$

where

K_s is the Effective Responsivity in (A/W), defined as

$$K_s = \frac{\int g(\lambda)S(\lambda)\mathrm{d}\lambda}{\int g(\lambda)\mathrm{d}\lambda} \tag{3.2}$$

where S(λ) is the absolute spectral response of a silicon cell (A/W) and g(λ) the irradiance spectrum (W/m$^2\mu$m);

G is the solar irradiance (W/m^2);

A is the irradiated active surface of the cell.

While the Spectral Response of the silicon is constant, the irradiance spectrum changes with the weather conditions and the day of the year. As an example, Figure 3.1 shows the quantities S(λ), g1(λ) and g2(λ) at 12.00 of a clear day in winter and summer, respectively. Figure 3.2 shows the quantities S(λ) $\cdot$ g1(λ) and S(λ)$\cdot$ g2(λ), named spectral current density δI$_1$ e δI$_2$, which have units of A/(m$^2\mu$m).

When the solar cell is not illuminated it behaves like a diode, so its current in dark conditions, named as dark current, is a function of the cell's voltage and

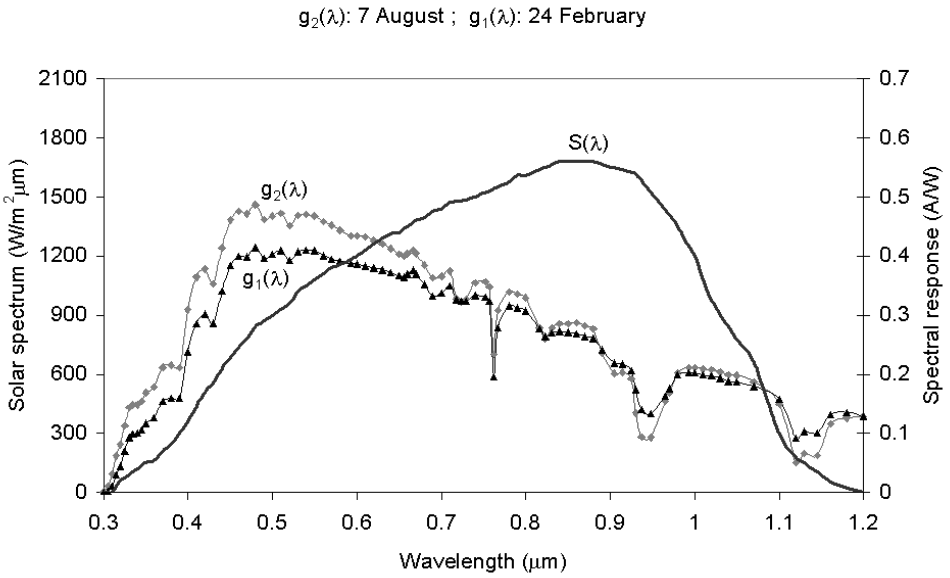

Figure 3.1: Comparison of solar spectra in winter and summer.

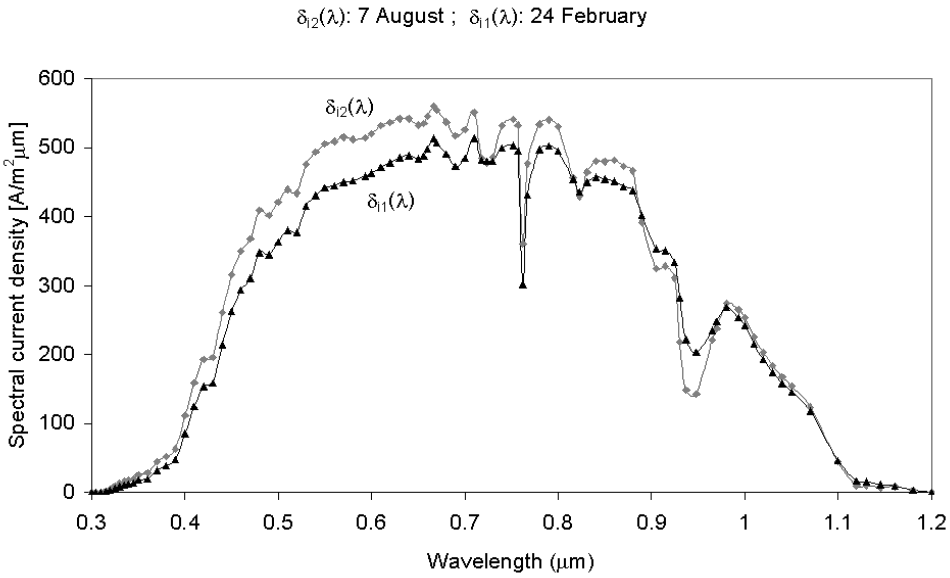

Figure 3.2: Comparison of spectral current density in winter and summer.

it is given by Shockley equation [47]

$$I_D = I_0\left[e^{\left(\frac{qV}{kT}\right)} - 1\right] \tag{3.3}$$

where

e is electron charge;

k is Boltzmann constant;

T is the temperature in K;

I_0 is the inverse saturation current of the diode.

The term kT/q is equal to the thermal voltage. As a first conclusion, in its basic form, the solar cell can be modelled by a current generator with a diode in parallel, as illustrated in Figure 3.3.

Therefore, the behavior of the solar cell can be described, in first approxima-

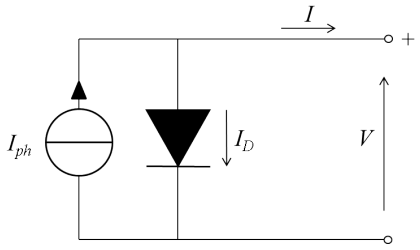

Figure 3.3: Single diode model for ideal solar cell.

tion, with the diode current-voltage (I-V) curve, offset from the origin by the photogenerated current I_{ph}, as illustrated in Figure 3.4 and reported in the 3.4 equation

$$I = I_{ph} - I_0\left[e^{\left(\frac{qV}{mkT}\right)} - 1\right] \tag{3.4}$$

where m is the ideality factor which is defined as how closely a diode follows its ideal characteristic. The value of m depends on recombination effects and it

can vary from 1 to 5 for different kinds of cell, even if a value between 1 and 2 is typical in practical cases for high and low voltages respectively [48]. In short

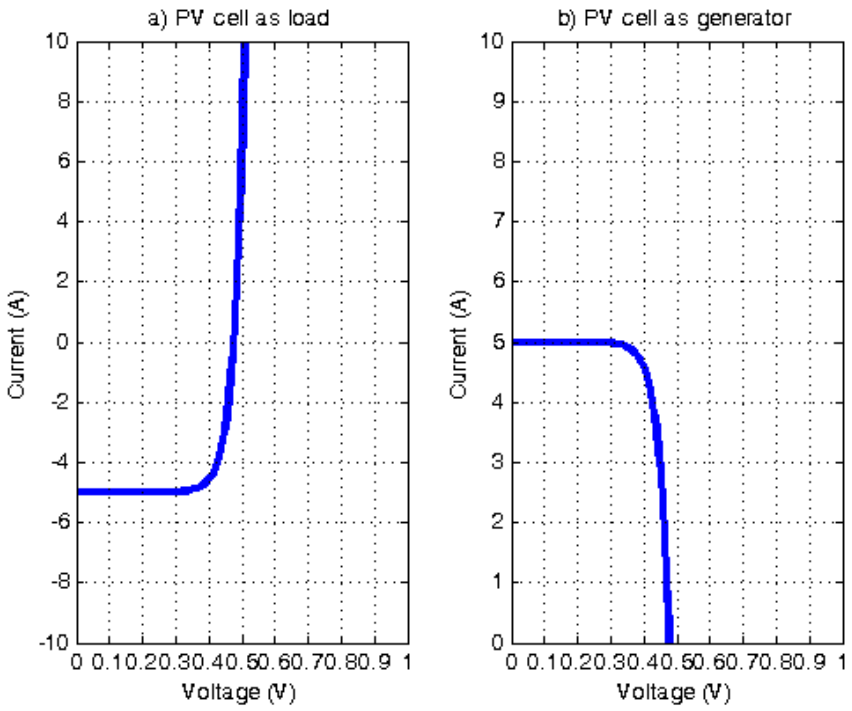

Figure 3.4: Ideal I-V curve of a solar cell: a) as a load in two quadrants; b) as generator only in the first quadrant.

circuit conditions (SC), the solar cell generates its maximum current I_{SC}, equal to I_{ph}, while in open circuit conditions the highest voltage V_{OC} is obtained. The V_{OC} is defined as the voltage at which the short circuit current equals the forward bias diffusion current with opposite polarity. According to Eq. 3.4 V_{OC} can be computed as

$$V_{OC} = \frac{mkT}{q} \ln\left(\frac{I_{ph}}{I_0} + 1\right) \tag{3.5}$$

The Maximum Power Point (MPP), at which the product of V and I is at a maximum P_m, is the optimal operating point of the solar cell. Voltage and current at P_m are V_m and I_m, respectively. It is obvious that the ideal solar cell has a characteristic that approaches a rectangle. The fill factor $FF = I_m V_m / I_{SC} V_{OC}$ should be close to one. In real devices, for very good crystalline silicon solar cells,

the fill factors are above 0.8 or 80%.
The solar cell current-voltage characteristic is highly dependent on the cell's temperature and solar irradiance level on its surface. The photogenerated current is linearly dependent on the solar irradiance G and increases slightly when the cell temperature T_c raises, while the open-circuit voltage highly changes with the temperature, with a opposite dependence respect to the solar cell current. As reference conditions for the PV generators, the Standard Test Conditions (STC) are defined as those where the solar irradiance G_{STC} is equal to 1000 W/m^2, the cell temperature T_{STC} is 25 ℃ and the Air Mass (AM) is 1.5. Equations 3.6 and 3.7 describe the I_{ph} and V_{OC} variation respect to the STC conditions

$$I_{ph} = I_{ph,STC}\frac{G}{G_{STC}}\Big[1 + \alpha(T_c - T_{STC})\Big] \tag{3.6}$$

$$V_{OC} = V_{OC,STC}\Big[1 + \beta(T_c - T_{STC})\Big] \tag{3.7}$$

where

α is the positive thermal coefficient of I_{ph} at STC (in %/K);

β is the negative thermal coefficient of V_{OC} at STC (in %/K).

As an illustrative example of the solar cell I-V and P-V curves modifications at different conditions respect to STC, Figures 3.5– 3.8 show the behaviour of a solar cell with $I_{ph,STC}$=5 A, $V_{OC,STC}$=0.6 V, α=0.06 $\%/K$ and β=−0.34 $\%/K$ at various temperatures and solar irradiance values.

The non-ideal nature of the solar cell imposes to modify the equivalent circuit adding other lumped components in order to consider some loss mechanisms. A parallel resistance R_{sh}, also called the shunt resistance, can be added in parallel to the dark current diode, with the aim to consider the current leakage due to dislocations, grain boundaries or microfractures in the base material, or metallic bridges formed by impurities introduces during diffusion processes in impure atmosphere or high temperature contact metallizations. These impurities decrease the resistance between p-type and n-type silicon in the area of the space charge, causing a drop in the photovoltage and the presence of a leakage current.
A series resistance R_s can represent the sum of the resistances of particular com-

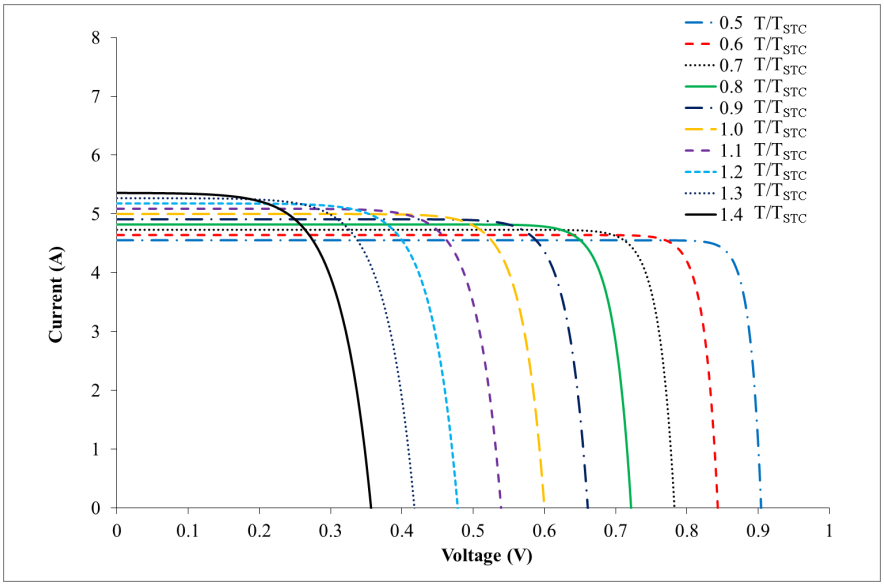

Figure 3.5: Effect of temperature on a solar cell I-V curve.

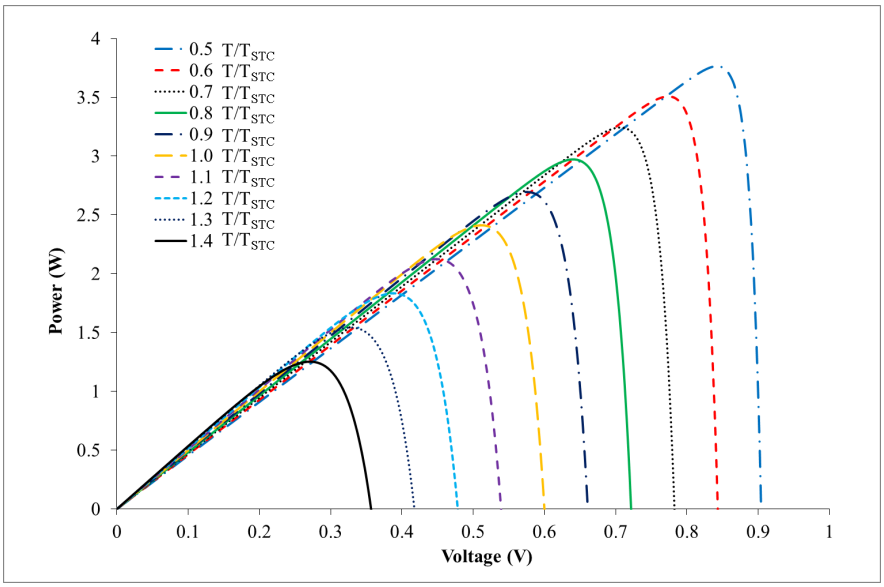

Figure 3.6: Effect of temperature on a solar cell P-V curve.

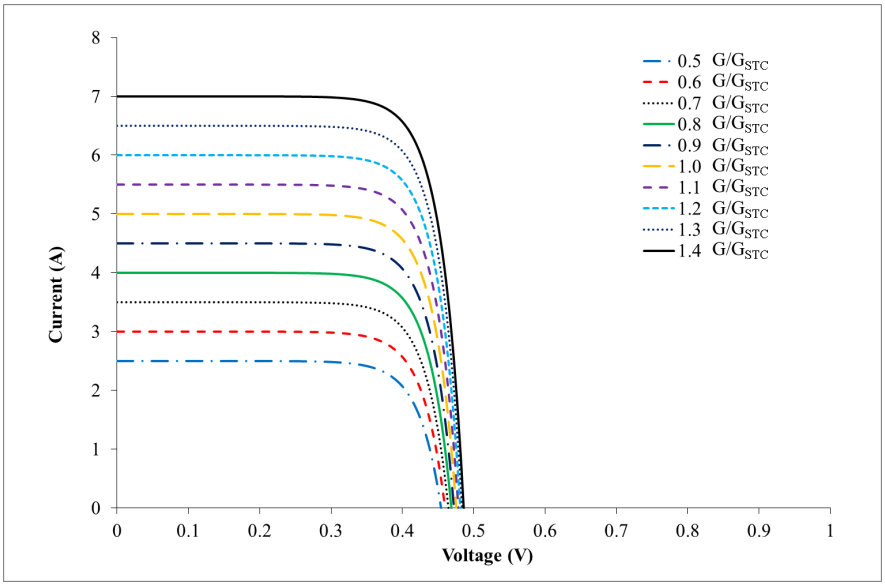

Figure 3.7: Effect of solar irradiance on a solar cell I-V curve.

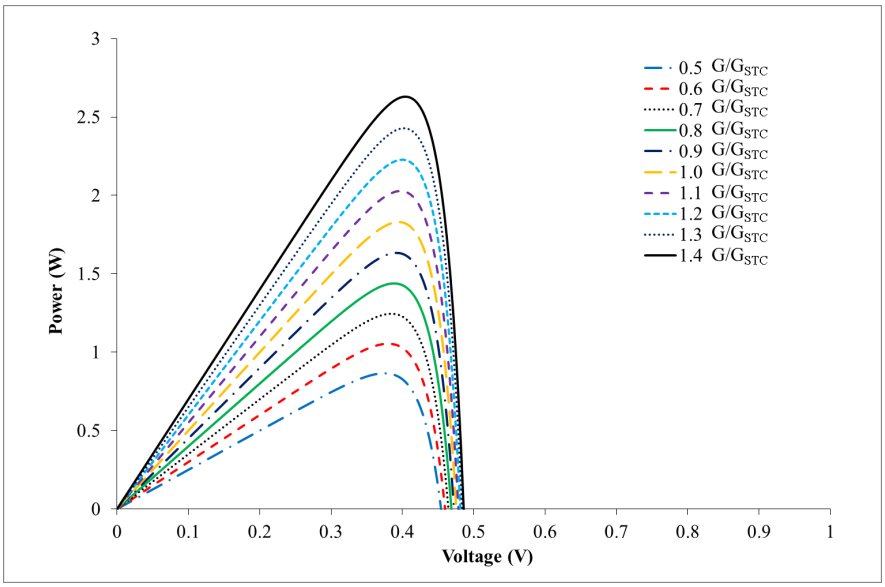

Figure 3.8: Effect of solar irradiance on a solar cell P-V curve.

ponents of the cell, such as the base material's contact to the rear electrode, the bulk material, the emitter material, the emitter's contact to the front electrode and the front electrode. The resistance of the rear contact, made of full metallic layer, should be considered as negligibly small.
If these components are incorporated in the model, the equivalent circuit in Figure 3.9 is obtained and the static characteristic of the solar cell becomes

$$I = I_{ph} - I_0\left\{e^{\left[\frac{q(V+IR_s)}{mkT}\right]} - 1\right\} - \frac{V+IR_s}{R_{sh}} \tag{3.8}$$

The effect of the R_{sh} and R_s on the I-V characteristic of the solar cell considered

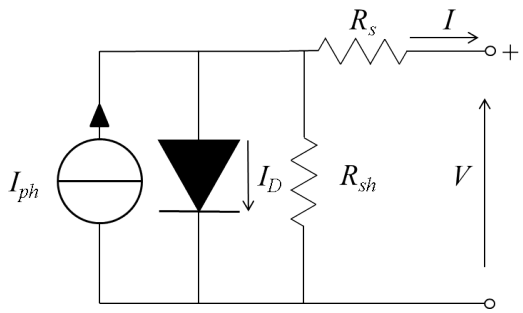

Figure 3.9: Single diode with series and parallel resistance equivalent circuit.

above, at STC, is illustrated in the Figures 3.10 and 3.11 respectively.

3.2 Parameters of the solar cell model

The circuit parameters I_{ph}, R_s, R_{sh}, I_0 and m at a certain solar irradiance and air temperature can be obtained by solving the governing equations of the solar cell [49] for the parameters values of V_{OC}, I_{SC}, V_m and I_m, which can be experimentally measured, and R_{sh0} and R_{s0}, which are defined as

$$R_{s0} = -\left(\frac{\mathrm{d}V}{\mathrm{d}I}\right)_{V=V_{OC}} \tag{3.9}$$

$$R_{sh0} = -\left(\frac{\mathrm{d}V}{\mathrm{d}I}\right)_{I=I_{SC}} \tag{3.10}$$

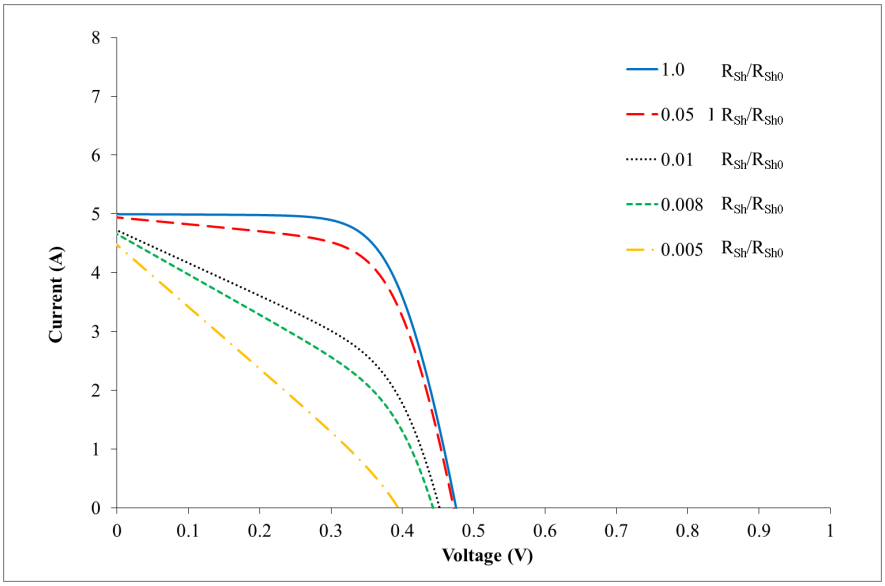

Figure 3.10: Effect of R_{sh} on a solar cell I-V curve (R_{sh0}=17 Ω).

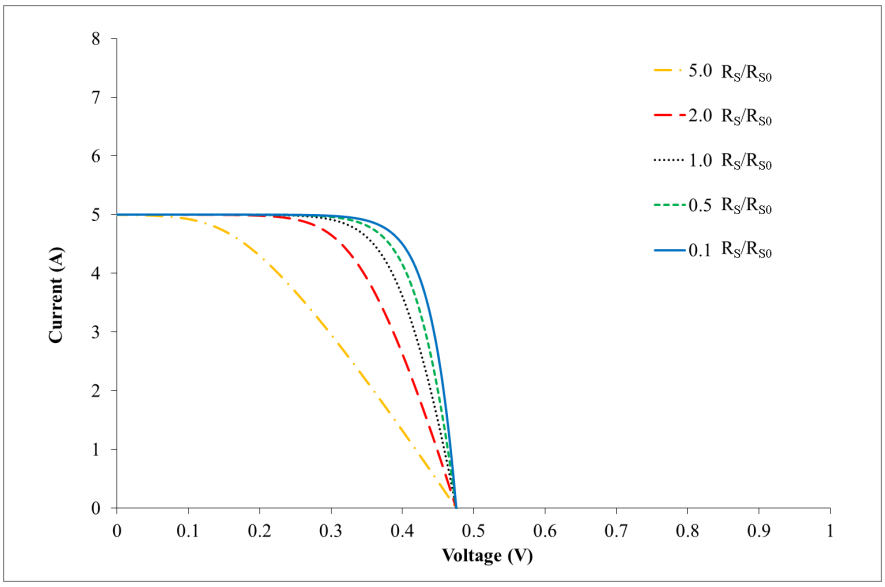

Figure 3.11: Effect of R_s on a solar cell I-V curve (R_{s0}=10 mΩ).

The five governing equations of the solar cell can be derived by 3.8 as described in the following. At the open circuit point on the experimental I-V curve $V = V_{OC}$ and $I = 0$, so substituting these conditions in 3.8 the first equation is

$$0 = I_{ph} - I_0\left[e^{\left(\frac{qV_{OC}}{mkT}\right)} - 1\right] - \frac{V_{OC}}{R_{sh}} \tag{3.11}$$

At the short circuit point $V = 0$ and $I = I_{SC}$. With these substitutions in 3.8 the second needed equation is

$$I_{SC} = I_{ph} - I_0\left[e^{\left(\frac{qR_s(I_{SC})}{mkT}\right)} - 1\right] - \frac{I_{SC}R_s}{R_{sh}} \tag{3.12}$$

If the derivative of 3.8 with respect to V is used

$$\frac{\mathrm{d}I}{\mathrm{d}V} = -I_0\left\{\frac{q}{mkT}\left(1 + \frac{\mathrm{d}I}{\mathrm{d}V}R_s\right)e^{\left[\frac{q(V+IR_s)}{mkT}\right]}\right\} - \frac{1}{R_{sh}}\left(1 + \frac{\mathrm{d}I}{\mathrm{d}V}R_s\right) \tag{3.13}$$

At the open circuit point on the I-V curve,

$$\frac{\mathrm{d}I}{\mathrm{d}V} = \left(\frac{\mathrm{d}I}{\mathrm{d}V}\right)_{V=V_{OC},I=0} = \left(-\frac{1}{R_{s0}}\right) \tag{3.14}$$

With this substitution in 3.13 the third needed equation is

$$-\frac{1}{R_{s0}} = -I_0\left[\frac{q}{mkT}\left(1 - \frac{R_s}{R_{s0}}\right)e^{\left(\frac{qV_{OC}}{mkT}\right)}\right] - \frac{1}{R_{sh}}\left(1 - \frac{R_s}{R_{s0}}\right) \tag{3.15}$$

At the short circuit point on the I-V curve,

$$\frac{\mathrm{d}I}{\mathrm{d}V} = \left(\frac{\mathrm{d}I}{\mathrm{d}V}\right)_{V=0,I=I_{SC}} = \left(-\frac{1}{R_{sh0}}\right) \tag{3.16}$$

With this substitution in 3.13 the fourth needed equation is

$$-\frac{1}{R_{sh0}} = -I_0\left[\frac{q}{mkT}\left(1 - \frac{R_s}{R_{sh0}}\right)e^{\left(\frac{qR_sI_{SC}}{mkT}\right)}\right] - \frac{1}{R_{sh}}\left(1 - \frac{R_s}{R_{sh0}}\right) \tag{3.17}$$

Finally, at any point on th I-V curve,

$$P = VI. \tag{3.18}$$

By differentiating 3.18 with respect to V,

$$\frac{\mathrm{d}P}{\mathrm{d}V} = \left(\frac{\mathrm{d}I}{\mathrm{d}V}\right) V + I \tag{3.19}$$

At the maximum power point $I = I_m$, $V = V_m$ and this derivative is zero, so

$$\frac{\mathrm{d}I}{\mathrm{d}V} = -\frac{I_m}{V_m} \tag{3.20}$$

Substituting 3.18 in 3.13 the fifth needed equation is defined

$$-\frac{I_m}{V_m} = -I_0\left\{\frac{q}{mkT}\left(1 - \frac{I_m}{V_m}R_s\right)e^{\left[\frac{q(V_m + R_s I_m}{mkT}\right]}\right\} - \frac{1}{R_{sh}}\left(1 - \frac{I_m}{V_m}R_s\right). \tag{3.21}$$

The equation system presented above can be resolved with the Newton-Raphson technique, but in literature other ways to obtain a solution are proposed, for example an alternative way to compute the equivalent parameters of the solar cell is through the following analytical expressions [50] derived from 3.11, 3.12, 3.15, 3.17 and 3.21

$$R_{sh} = R_{sh0} \tag{3.22}$$

$$m = \frac{V_m + R_{s0}I_m - V_{OC}}{\frac{kT}{q}\left[\ln\left(I_{SC} - \frac{V_m}{R_{sh}} - I_m\right) - \ln\left(I_{SC} - \frac{V_{OC}}{R_{sh}}\right) + \frac{I_m}{I_{SC} - (V_{OC}/R_{sh})}\right]} \tag{3.23}$$

$$I_0 = \left(I_{SC} - \frac{V_{OC}}{R_{sh}}\right) e^{\left(-\frac{qV_{OC}}{mkT}\right)} \tag{3.24}$$

$$R_s = R_{s0} - \frac{mkT}{qI_0} e^{\left(-\frac{qV_{OC}}{mkT}\right)} \tag{3.25}$$

$$I_{ph} = I_{SC}\left(1 + \frac{R_s}{R_{sh}}\right) + I_0\left(e^{-\frac{qI_{SC}R_s}{mkT}} - 1\right) \tag{3.26}$$

Other authors [51] have prosed some analytical manipulations in order to obtain an explicit form for the current in function of the voltage and to compute R_s and R_{sh}, using the LambertW [52] function.

In the next section the experimental method used in this dissertation to determine the solar cell's equivalent circuit parameters from the I-V curve of a PV generator is exposed.

3.3 Parameters' evaluation from experimental measurements

The I-V characteristic of a PV generator, either a solar cell, a panel or a complex array can be reconstructed experimentally acquiring the current and voltage across its terminals while it is energizing a variable load, such as an electronic load. In all the experimental work for this thesis it has been used the method of the external capacitor charging [53], in which all the points of the PV generator I-V characteristic are sweeped from short circuit conditions to open circuit ones, during the charge of a capacitor used as load.

3.3.1 Experimental setup and measurements

In Figure 3.12 is illustrated the layout of the measuring circuit. When the switch is closed, the voltage signal is acquired by a differential probe, while for the current a probe based on Hall effect is used. The signal conditioning and Data Acquisition (DAQ) are performed by a dedicated board connected to the PC via USB interface. On the computer custom LabVIEW™virtual instruments run to perform the functions of oscilloscope and recording data.
In particular, the list of instruments necessary for this kind of measure is reported below

- Acer TravelMate 5720 PC laptop.
- National Instruments NI USB-6251 BNC Board, with a 16-bit analog/digital converter and a maximum sampling rate of 1.25 MSa/s.

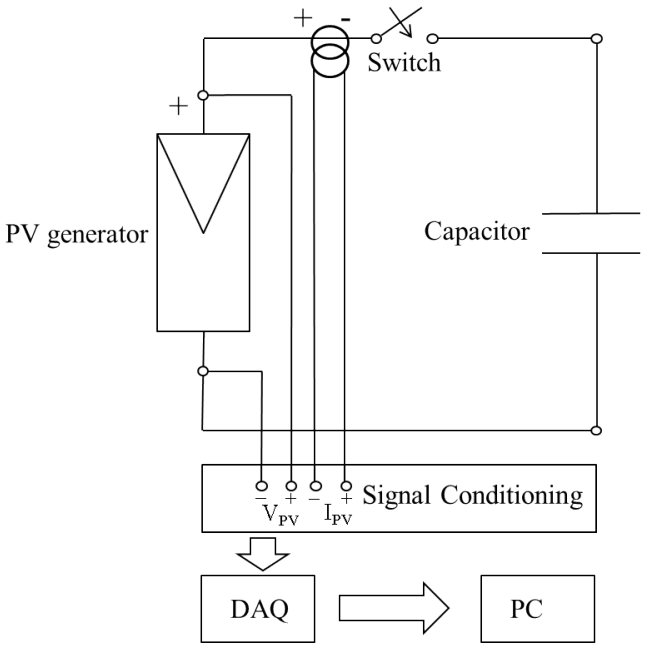

Figure 3.12: I-V curve measuring circuit.

- TiePie SI-9002 differential probe, characterizated by: two attenuation rates (1:20 for a maximum voltage of 140 V_{rms} or 1:200 for 1400 V_{rms} maximum voltage); DC to 25 MHz bandwidth; ±2% accuracy.
- 2 Lem PR30 DC/AC current probe, based on Hall effect, characterizated by: 20 A_{rms} maximum current (± 30 A of peak value); DC to 100 kHz bandwidth; ±1% accuracy.
- Tritec Energie Spektron 100 mono-crystalline silicon solar irradiance sensor, calibrated by JRC ESTI[1] Lab in Ispra (Varese, Italy), with traceability to Fraunhofer Institute for Solar Energy Systems (ISE) in Freiburg (Germany).
- IKS Photovoltaik ISET poly-crystalline silicon solar irradiance sensor, with traceability to Fraunhofer Institute for Solar Energy Systems (IWES) in Kassel (Germany).
- 10 mF capacitor.

[1]Joint Research Centre (JRC) European Solar Test Installation

- Thermometer based on thermistor.

It is worth noting that the final uncertainties of voltage, current and power are improved by repetitive calibration in laboratory. As an example, a 240 W_p polycristalline silicon (p-Si) PV module, made of 60 cells, is considered. In Figure 3.13 the settings of the virtual instrument are illustrated, while in Figure 3.14 the physical quantities acquired are represented, together with the resulting I-V curve at the experimental conditions (G=764 W/m^2 and T_{air}=28 °C).

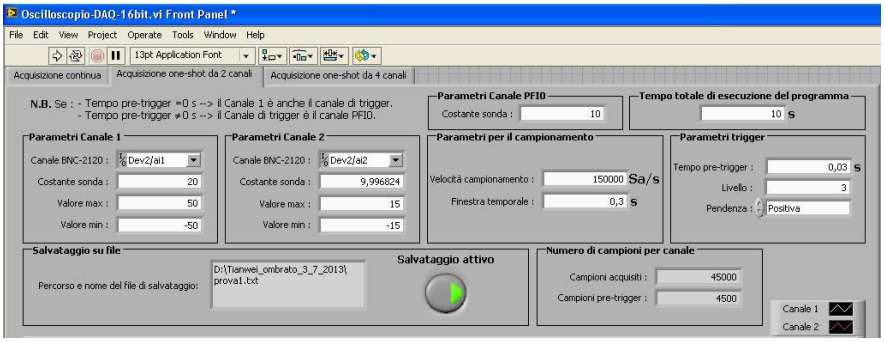

Figure 3.13: Settings of the virtual instrument.

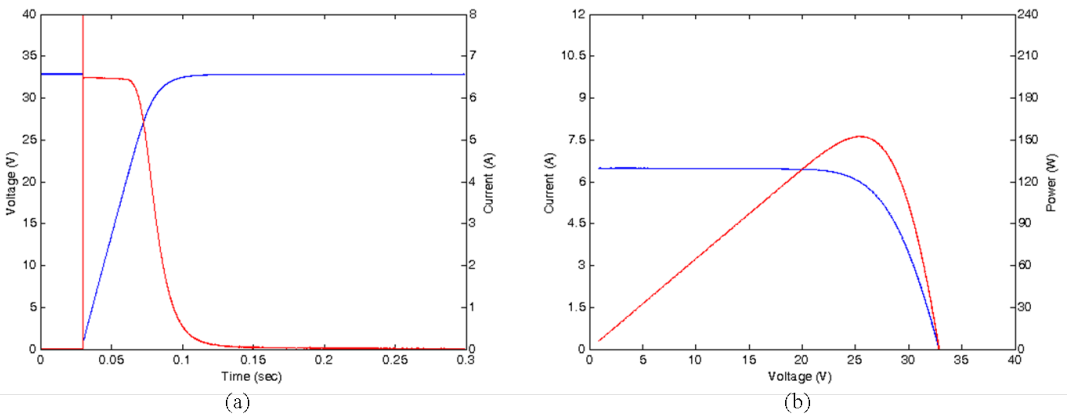

Figure 3.14: (a) Voltage (blue curve) and current (red curve) generated by the 240 W_p p-Si module during the capacitor charging. (b) Current-voltage and power-voltage curve of the 240 W_p p-Si module at experimental conditions.

3.3.2 Post-processing and parameter evaluation

From the I-V curve in Figure 3.14(b), applying the definitions 3.9 and 3.10, the parameters R_{s0} and R_{sh0} can be determined from the angular coefficients of the tangent lines of the I-V curve at the open circuit and short circuit points respectively, as illustrated in Figure 3.15. The tangent line at the short circuit point gives also the value of the I_{SC}, while the open circuit voltage V_{OC} is determined from the voltage values before the trigger of the measurement. V_m and I_m at the MPP are extracted directly from the data.

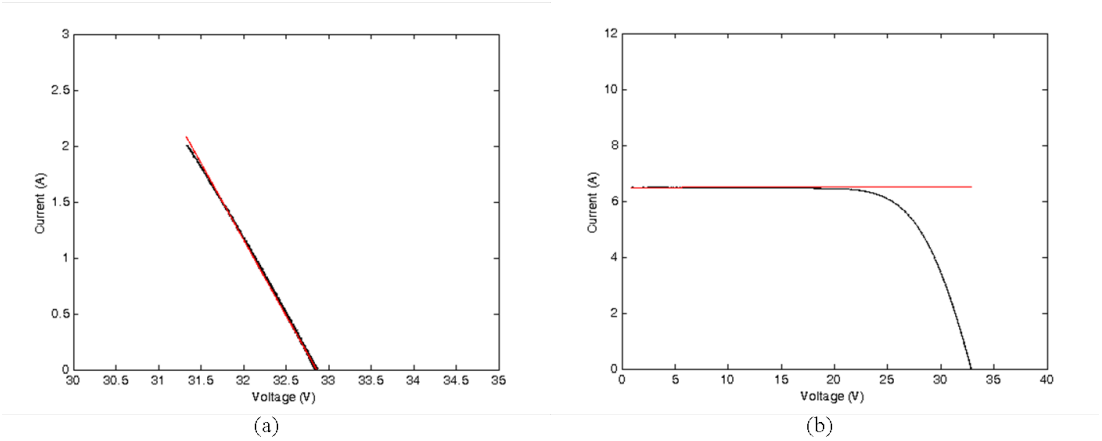

Figure 3.15: (a) R_{s0} computation and (b) R_{sh0} and I_{SC} extrapolation.

The Table 3.1 reports the parameters extracted from the I-V curve at the experimental conditions (G=764 W/m^2 and T$_c$=53.7 °C)

The values of R_{s0} and R_{sh0} are used as initial guess for R_s and R_{sh}, while for the ideality factor m an suitable initial hypothesis is assumed in the range 1–1.3. Therefore, the initial values of I_0 and I_{ph} are computed from Eq. 3.11 and 3.12 respectively, as reported below

$$I_0 = \frac{I_{SC} - \frac{V_{OC}}{R_{sh}}}{e^{\left(\frac{qV_{OC}}{mkT}\right)} - 1} \tag{3.27}$$

Parameter	Value	
$\mathbf{I_{SC}}$	6.49	A
$\mathbf{V_{OC}}$	32.85	V
$\mathbf{P_m}$	152.51	W
$\mathbf{I_m}$	5.94	A
$\mathbf{V_m}$	25.68	V
$\mathbf{R_{s0}}$	0.74	Ω
$\mathbf{R_{sh0}}$	868.	Ω

Table 3.1: PV module's experimental parameters.

imposing at this stage that I_{ph}=I_{SC},

$$I_{ph} = I_{SC}\left(1 + \frac{R_s}{R_{sh}}\right) + I_0\left[e^{\left(\frac{qR_sI_{SC}}{mkT}\right)} - 1\right] \tag{3.28}$$

At this point, the values of m and I_0 are refined through the formula 3.5 and 3.27, to impose the passage of the modelled I-V characteristic for V_{OC}. Thus, the values of R_s and then R_{sh} are adjusted to satisfy 3.15 and 3.17

$$R_s = \frac{\frac{1}{R_{sh0}} - \frac{1}{R_{s0}} + \frac{qI_0}{mkT}e^{\left(\frac{qV_{OC}}{mkT}\right)}}{\frac{qI_0}{mkTR_{s0}}e^{\left(\frac{qV_{OC}}{mkT}\right)} + \frac{1}{R_{sh0}R_{s0}}} \tag{3.29}$$

$$R_{sh} = \frac{1 - \frac{R_s}{R_{sh0}}}{\frac{1}{R_{sh0}} - I_0\left[\frac{q}{mkT}\left(1 - \frac{R_s}{R_{sh0}}\right)e^{\left(\frac{qR_sI_{SC}}{mkT}\right)}\right]} \tag{3.30}$$

Finally also the I_{ph} can be re-computed with 3.28 using the new values for R_s, R_{sh}, m and I_0. The Table 3.2 reports the parameters of the single diode model for a solar cell as computed from the experimental measurement on a 240 W_p PV module at the experimental conditions (G=764 W/m^2 and T_c=53.7 °C)

Once the solar cell parameters are known, the I-V characteristic of any PV generator composed by a number of those series connected cells can be reconstructed and compared to that from experimental data to evaluate the goodness of the

Parameter	Value	
$\mathbf{I_{ph}}$	6.50	A
$\mathbf{I_0}$	1.35 x $10^{-}7$	A
m	1.10	W
$\mathbf{R_{sh}}$	14.38	Ω
$\mathbf{R_s}$	7.48	mΩ

Table 3.2: Solar cell single diode model parameters at experimental conditions.

model. The Fig. 3.16 illustrates the current-voltage and power-voltage curves of the model together with the experimental data for the I-V characteristic and the ideal diode model I-V curve (without R_s and R_{sh}), for the case described above. The RMSD[1] results to be equal to 0.028 A, which is a good fitting of the real

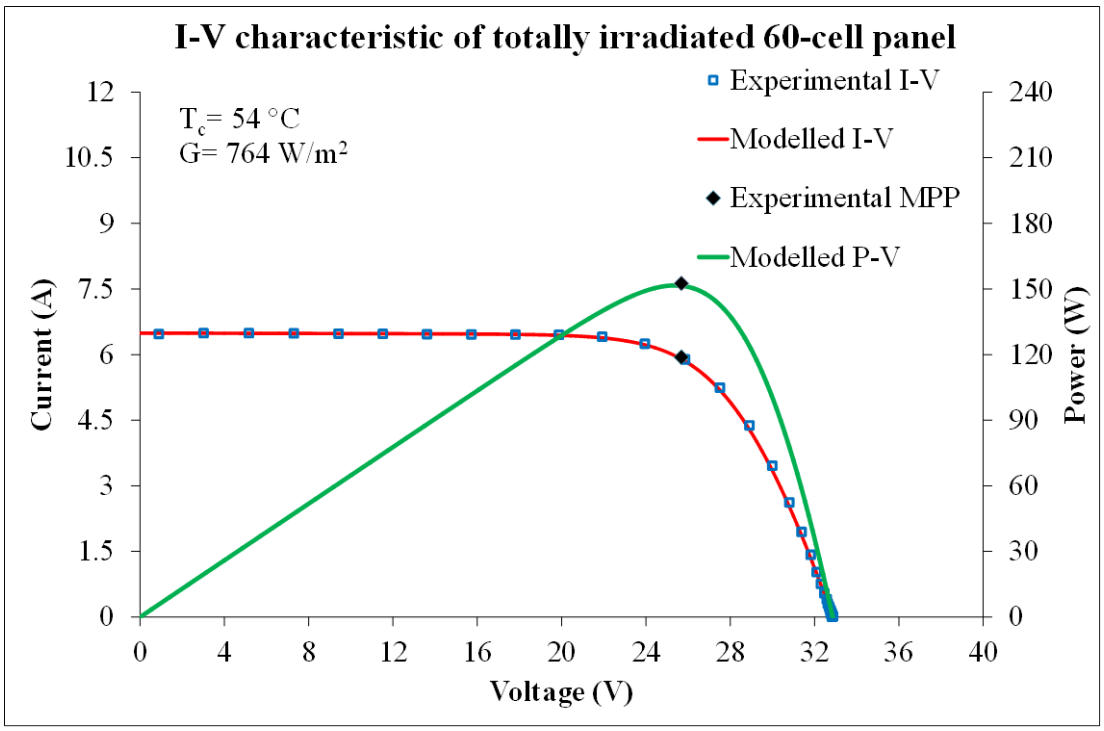

Figure 3.16: I-V curves comparison.

[1]Root Mean Square Deviation

curve, as can be seen from the figure.
These results allow some considerations about the influence of R_s and R_{sh} on the deviation of the I-V curve from the ideal shape. According to [54] it is possible to reconstruct the Fill Factor of a resistance-free cell, expressing the voltage and current at MPP of a solar cell as

$$V_{mpp} = V_0 - I_{mpp}R_s \tag{3.31}$$
$$I_{mpp} = I_0 - (V_{mpp} + I_{mpp}R_s)/R_{sh} \tag{3.32}$$

and finding the product $V_0 I_0$, normalized with $V_{OC}I_{SC}$

$$FF_0 = FF + \frac{I_{mpp}^2 R_s}{V_{OC}I_{SC}} + \frac{(V_{mpp} + I_{mpp}R_s)^2}{R_{sh}V_{OC}I_{SC}} = FF + \Delta FF_{R_s} + \Delta FF_{R_{sh}} \tag{3.33}$$

This supposes the approximation that V_0 and I_0 are the MPP of the resistance-free cell, meaning that R_s only shifts V_{mpp} and R_{sh} only shifts I_{mpp}. This is acceptable if the relative errors in ΔFF_{R_s} and $\Delta FF_{R_{sh}}$ are less than 5%, which can be obtained for R_s<4Ωcm^2 and R_{sh}>50Ωcm^2, as in the case discussed. From the cell parameters computed it is obtained a ΔFF_{R_s} equal to 0.074 and a $\Delta FF_{R_{sh}}$ of 0.004, which summed to the FF (0.71) from the values of Table 3.1 give a FF_0 equal to 0.79, the same obtained from the I-V curve of the ideal model of Fig. 3.16.
It can be stated, in this case, that for a PV module totally irradiated, without shade or other degradation phenomena, the main contribution to the Fill Factor losses is given by the R_s.
In order to be able to compare different characteristics acquired in whatever experimental conditions, it is possible to translate the I-V curve at the Standard Test Condition (STC), according to EN 60891 [55]

$$I_{STC} = I_{measured} + I_{SC}\left(\frac{G_{STC}}{G} - 1\right) + \alpha\Delta T \tag{3.34}$$
$$V_{STC} = V_{measured} - Rs\,(I_{STC} - I_{measured}) - KI_{STC}\Delta T + \beta\Delta T \tag{3.35}$$

where

ΔT is equal to 25 ℃ - T_c;

K is a parameter equal to 2 mΩ/℃.

The Table 3.3 reports the parameters extracted from the I-V curve at the STC conditions

Parameter	**Value**	
$\mathbf{I_{SC}}$	8.35	A
$\mathbf{V_{OC}}$	36.06	V
$\mathbf{P_m}$	215.17	W
$\mathbf{I_m}$	7.64	A
$\mathbf{V_m}$	28.19	V

Table 3.3: PV module's parameters at STC.